J Mater Sci: Mater Med (2007) 18:1071–1077
DOI 10.1007/s10856-007-0137-y

Novel hydroxyapatite (HA) dual-scaffold with ultra-high porosity, high surface area, and compressive strength

In-Kook Jun · Young-Hag Koh · Su-Hee Lee · Hyoun-Ee Kim

Received: 2 September 2005 / Accepted: 29 March 2006 / Published online: 1 February 2007

Abstract A novel scaffold designed for tissue engineering applications, which we refer to as a ''dual-scaffold'' because its structure consists of two interlaced three-dimensional (3-D) hydroxyapatite (HA) networks, was fabricated using a combination of the rapid prototyping (RP) method and dip-coating process. To accomplish this, a graphite network acting as a template was prepared using the RP method and then uniformly dip-coated with HA slurry. The resultant sample was then heat-treated at 1250 °C for 3 h in air to remove the graphite network and consolidate the HA networks. An additional 3-D channel was formed by removing the graphite network, while preserving the pre-existing channel. The unique structure of the dual-scaffold endows it with unprecedented features, such as ultra-high porosity (>85%), a high surface area and high compressive strength, as well as a tightly controlled pore structure. In addition, an excellent cellular response was observed to the fabricated HA dual-scaffold.

Introduction

Bioceramic scaffolds have attracted a great deal of attention in the tissue engineering field, since their 3-D open pores and biocompatible surfaces are beneficial to the growth of cells and tissue differentiation [1–6]. When bioactive materials are implanted in the body, they form a bond with the tissue, due to their elicitation of a specific biological response at the interface between the two substances [7]. In terms of the structure of the scaffold, it should preferably have a high porosity, a high surface area, an interconnection, and high structural stability [8].

Bioceramic scaffolds with different structures and various functionalities have been fabricated, including foam [9] and 3-dimensional networks [10]. For example, ceramic foam is comprised of thin struts, and is commonly fabricated by coating an open-cell polymeric foam with a ceramic slurry, followed by pressureless sintering at elevated temperatures [9, 11, 12]. This method of fabrication allows the ceramic foam to be imbued with an ultra-high porosity, e.g. >85%, without difficulty; however, it provides only limited control over the different aspects of the pore structure, such as the pore size, shape, and interconnection.

On the other hand, a simple 3-D ceramic network comprised of rectangular prisms can be readily fabricated by the rapid prototyping (RP) method [10, 13–16]. The RP method allows 3-D objects to be rapidly constructed layer-by-layer using the data generated by CAD systems. Several RP methods have been successfully employed to create bioceramic scaffolds by directly depositing a ceramic loaded feedstock through a fine nozzle [10, 13]. However, the processing difficulties associated with this technique have led to the more widespread use of indirect RP for the fabrication of ceramic scaffolds. In the case of the indirect RP method, a polymeric scaffold used as a template is prepared by the direct RP method, and then cast with a highly loaded ceramic slurry, followed

I.-K. Jun · Y.-H. Koh (✉) · S.-H. Lee · H.-E. Kim
School of Materials Science and Engineering, Seoul National University, Seoul 151-742, Korea
e-mail: kohyh@snu.ac.kr

by heat-treatment [14, 15]. Even though both methods allow good control over the pore structure, it is very difficult to achieve ultra-high porosity, because of the necessity to construct very thin ceramic plates instead of columns.

Therefore, in this study, we describe the novel structure of scaffold, referred to as a 'dual-scaffold', in order to overcome the limitations associated with traditional scaffolds. More specifically, a traditional scaffold consists of a simple 3-D network comprised of straightforward ceramic plates or columns, in which only one 3-D channel (channel I) directs the growth of the cells, as shown in Fig. 1(A). On the other hand, the dual-scaffold is comprised of very thin ceramic plates, as shown in Fig. 1(B). This dual-scaffold fundamentally mimics the structure of the 3-D network; however the key difference is that a second channel (channel II) is formed inside the ceramic networks, in addition to the pre-existing channel (channel I). This process allows the dual-scaffold to have an ultra-high porosity, a high surface area, and structural stability, as well as a controlled pore structure.

To implement this novel design, we fabricated and characterized hydroxyapatite (HA: $Ca_{10}(PO_4)_6(OH)_2$) dual-scaffolds with various degrees of porosity. The samples were fabricated by coating the 3-D graphite network with the HA slurry, followed by heat-treatment at 1250 °C for 3 h. This produced an addition 3-D channel as a replica of the graphite network, while preserving the pre-existing channel. The fabricated dual-scaffolds were characterized in terms of their porosity, surface area, and pore structure. In order to evaluate their structure integrities, compressive strength tests were conducted for the samples. In addition, the cellular responses to the samples were characterized.

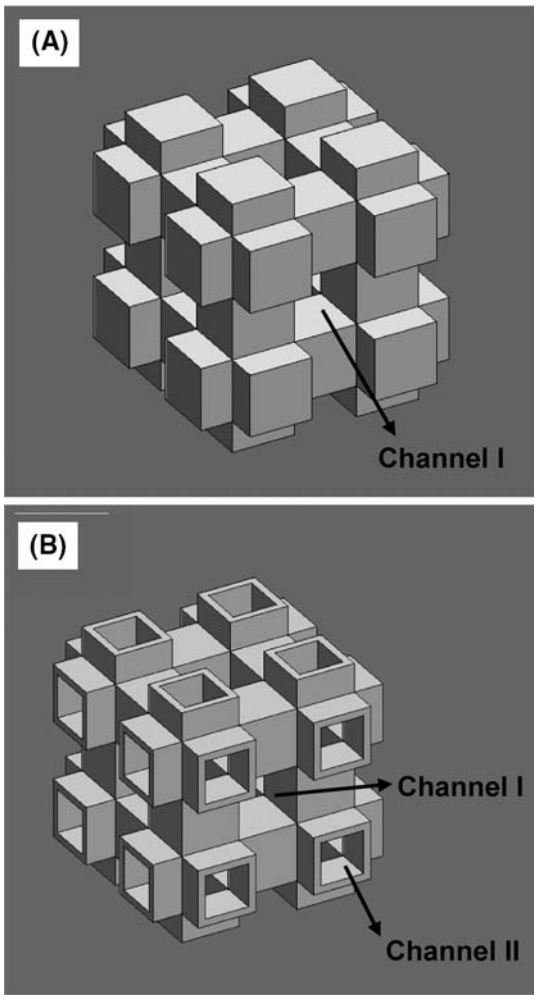

Fig. 1 Schematics of (**A**) a simple scaffold that has one 3-D channel (channel I), and (**B**) a dual-scaffold, in which an additional channel (channel II) is formed inside the 3-D network

Experimental procedure

3-D graphite network fabrication

Commercially available graphite (Tokai Crabon Co. Ltd, Tokyo, Japan) was selected for the fabrication of the template, because it can be completely removed via thermal oxidation. Graphite plates with dimensions of $15 \times 15 \times 1.4$ mm were bi-axially machined using a mini-CNC machine (Modela; Roland DGA Corp., Hamamatsu, Japan) in accordance with a predetermined CAD design to create periodic straight channels with size of 700×700 μm in the x–y plane and cylindrical channels with a diameter of 700 μm in the z-direction. The machined plates were laminated by applying polyvinylbutyl (PVB, Aldrich, USA) as a glue to produce permanent bonding between the lamina, creating a 3-D graphite network.

HA slurry preparation

Commercially available hydroxyapatite (HA) powder ($Ca_{10}(PO_4)_6(OH)_2$; Alfa Aesar Co., Milwaukee, WI) was selected because of its excellent biocompatibility. The as-received HA powder was calcined at 900 °C for 1 h in air to improve the rheological behavior of the HA slurry, by reducing its specific surface area [17]. The HA powder was dispersed in ethanol containing a predetermined amount of polyvinylbutyl and triethyl phosphate (TEP; $(C_2H_5)_3PO_4$, Aldrich, USA) acting as a binder and dispersant, respectively. The mixture was then ball-milled with ZrO_2 balls as the media for 24 h

to achieve a stable slurry with a homogenous distribution of the HA powders.

Fabrication of the HA dual-scaffold

The 3-D graphite network, fabricated by the RP method, was immersed in the HA slurry and subsequently blown with an air gun to uniformly coat its surface without blocking the channels. The HA-coated graphite network was dried at 70 °C for 12 h to ensure high green strength by removing the solvent. The outmost surface of the sample was ground to remove the HA coating layer, in order to reveal two pore channels, and then heat-treated at 1250 °C for 3 h in air to completely remove the graphite and consolidate the HA networks. An additional 3-D channel was formed by removing the graphite network, while preserving the pre-existing channel. The porosity of the dual-scaffold was able to be controlled by adjusting the number of replication cycles.

Characterization

The fabricated HA dual-scaffolds with various degrees of porosity were characterized using several analytical tools. The porosity of the sample was calculated by measuring its dimensions and weight. The surface area/volume was calculated by considering various geometrical factors, such as the pore size, porosity, and dimensions of the HA network. The macro-and microstructures of the sample were examined with optical microscopy (PMG3, Olympus, Tokyo, Japan) and scanning electron microscopy (SEM, JSM-6330, JEOL Technics, Tokyo, Japan).

Compressive strength measurement

For the compressive strength test, the HA dual-scaffolds were loaded at a crosshead speed of 10 mm/min using a screw driven load frame (Instron 5565, Instron Corp., Canton, MA) equipped with a 5 kN load cell. During the compressive strength tests, the stress and strain responses of the samples were monitored. Five samples were tested to obtain the average value along with its standard deviation.

In vitro cellular assay

The cellular response to the HA dual-scaffold was evaluated, in order to investigate the possible use in tissue engineering. Osteoblast-like MG63 cells were used after culturing them in flasks containing Dulbecco's modified Eagle's medium (DMEM, Life Technologies Inc., MD, USA) supplemented with 10% fetal bovine serum (FBS, Life Technologies Inc., MD, USA). The cells were then plated at a density of 1×10^4 cells/ml on a 24-well plate, containing the sample, and cultured for 1 day in an incubator humidified with 5% CO_2/ 95% air at 37 °C. The morphologies of the proliferated cells on the sample were observed with SEM after fixation with glutaraldehyde (2.5%), dehydration with graded ethanols (70, 90, and 100%), and critical point drying in CO_2.

Results and discussion

Fabrication of 3-D graphite network

For the fabrication of the dual-scaffold, we employed a combination of the RP method and dip-coating process. First, the graphite scaffold used as a template was prepared by the RP method, as shown in Fig. 2(A). Two different types of channel (square and cylindrical

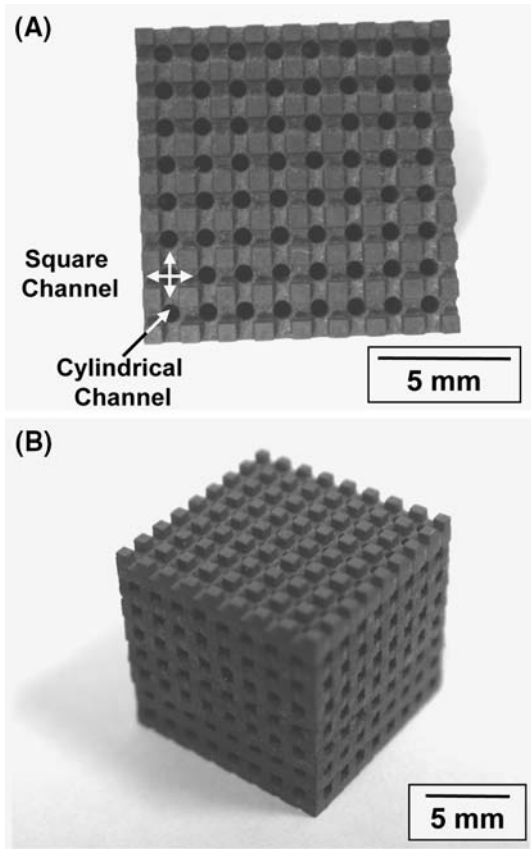

Fig. 2 Optical micrographs illustrating (**A**) a machined graphite plate and (**B**) a fabricated 3-D graphite network after laminating the pre-machined plates

channels) are visible in this figure. The original structure of the dual-scaffold consists of symmetric square channels following a 3-D periodic pattern; however, we modified the design, in order to be able to fabricate the 3-D graphite network more effectively. More specifically, straight square channels were formed in the x–y plane, while cylindrical channels were formed in the z direction. A simple 3-D graphite network was obtained by laminating the pre-machined graphite plates, so as to create one 3-D interconnected channel, as shown in Fig. 2(B). Only a small variation was observed in the sizes of the channels and graphite networks, meaning that the pore structure of the dual-scaffold was able to be precisely controlled.

Characterization of fabricated dual-scaffold

The 3-D graphite network was uniformly dip-coated with HA slurry, and then subjected to heat-treatment. It was observed that the graphite scaffold and organic binder in the ceramic coating layer are able to completely removed, without generating any noticeable defects in the sintered dual-scaffold. The fabricated HA dual-scaffold exhibited excellent shape tolerance, without distortion or cracking, as shown in Fig. 3(A). An additional 3-D channel was newly formed by removing the graphite scaffold, while preserving the pre-existing channel, in such a way that it was identical to the original design (Fig. 1B). A linear shrinkage of ~24% was observed after sintering at 1250 °C for 3 h in air. The formation of two periodic channels with the HA networks can be more clearly observed in the plane view shown in Fig. 3(B), where the square and cylindrical channels represent the additional and pre-existing channels, respectively. Each channel was interconnected in a 3-D pattern. An excellent pore structure was obtained, owing to the unique advantages of the RP method. We fabricated three kinds of HA dual-scaffolds with porosities of 87, 92 and 95%, respectively, by simply adjusting the number of replication cycles.

Figure 4(A) shows a typical SEM micrograph of the fracture surface of the HA network. Even though some pores are visible, the coating layer was well constructed, owing to the advantages of the ceramic

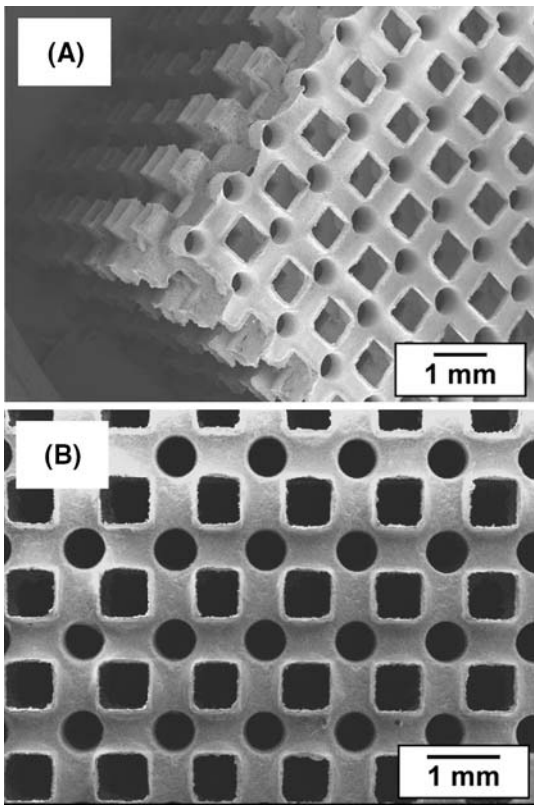

Fig. 3 SEM micrographs of a fabricated dual-scaffold illustrating (**A**) a 3-D image at low magnification and (**B**) two periodic channels in the plane view

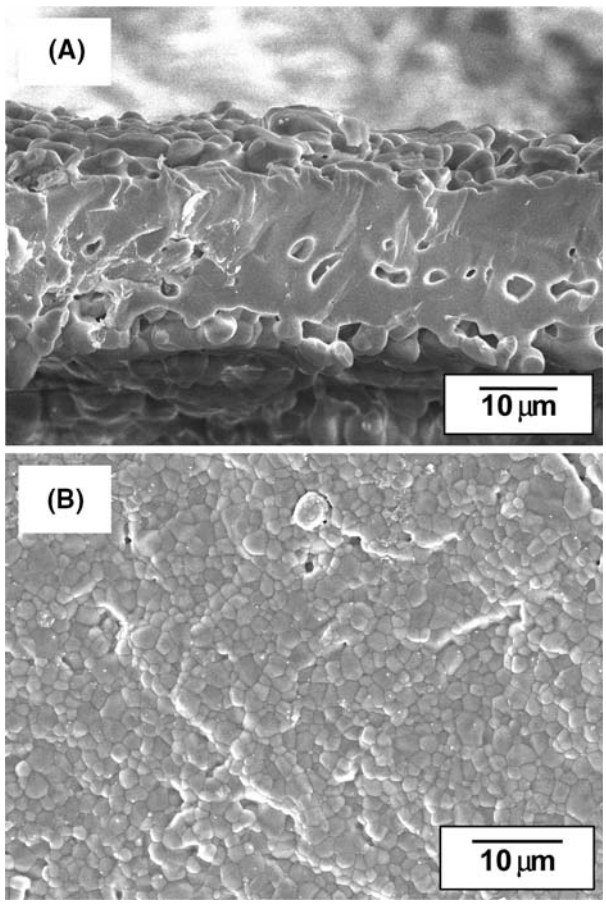

Fig. 4 Typical SEM micrograph of the HA dual-scaffold showing (**A**) the fracture surface of HA network and (**B**) the densification on the free surface

dip-coating process and the removal of the graphite scaffold used as a template via thermal oxidation. The thickness of the coating layer was found to linearly increase from 24 to 43 μm with increasing number of replication cycles. Good densification on the free surface of the HA network was observed in the SEM micrograph, along with a very fine grain size (Fig. 4B). These results indicate that the porosity of the dual-scaffold can be controlled without deteriorating the densification of the HA network, by simply adjusting the number of replication cycles.

Compressive strength

In order to evaluate the mechanical properties of the HA dual-scaffolds with various degrees of porosity, compressive strength tests were conducted. Most of the samples failed due to the vertical cracking, as shown in Fig. 5 which ensued when the tensile stress generated by the compression exceeded the strength of the material. In this case, the cracks propagated through the sample in a direction which was parallel to the loading direction, splitting it into parts. A similar failure mode was reported for porous ceramics with periodic pore structures [18]. However, in this previous case, lamina cracking was also observed during compression, in which the cracks were generated on the upper part of the sample and propagated through the plane that was normal to the loading direction. In this case, the major deformation mode of the sample is considered to be the bending of the ceramic networks, in the same manner that ceramic foams fail [19, 20].

A typical stress versus strain response during the compression of the HA dual-scaffold with a porosity of 87% is shown in Fig. 6. As first, the stresses increased linearly with elastic response, but then rapidly decreased due to fast fracture. The measured compressive strength was as high as 1.75 MPa. Even though there are many factors affecting the compressive strength of the sample, it is much higher than the corresponding value (0.16 ± 0.04 MPa) which was measured for an HA foam with similar porosity [21].

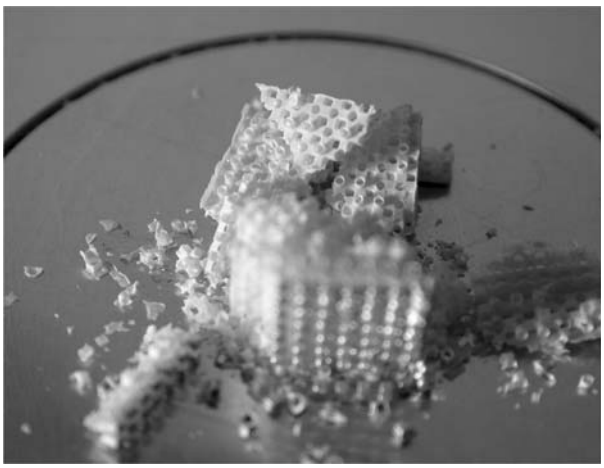

Fig. 5 Typical optical micrograph of the fractured HA dual-scaffold after compressive strength test illustrating the vertical cracking of the sample

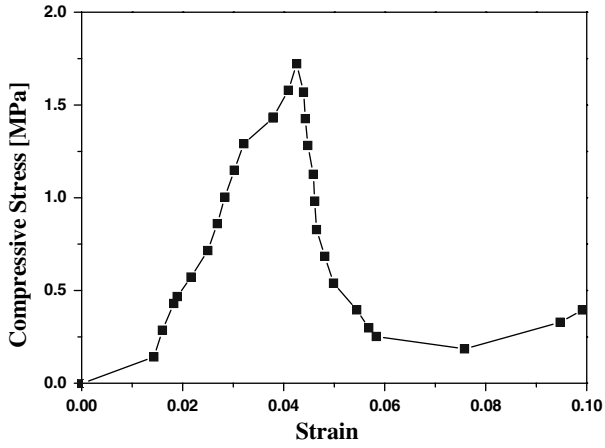

Fig. 6 Typical stress versus displacement response during compression of the HA dual-scaffold

The compressive strengths of the HA dual-scaffolds with various degrees of porosity are shown in Fig. 7. The measured value decreased from 1.56 to 0.18 MPa as the porosity was increased from 87 to 95%. It is not possible to directly compare these values with those of other reports, because of the unique pore structure of the HA dual-scaffolds. However, it is believed that the HA dual-scaffolds have high compressive strength at given porosity and pore size, owing to the controlled structure of the two interlaced networks.

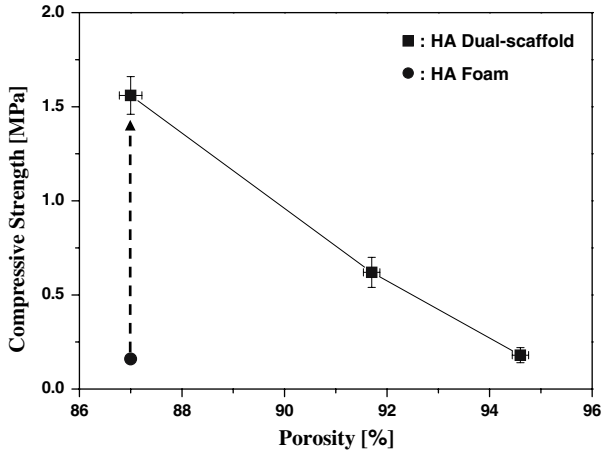

Fig. 7 Compressive strengths of the HA dual-scaffolds with various degrees of porosity

Cellular responses

In order to evaluate the possibility of using the HA dual-scaffold for tissue engineering, the cellular responses to the sample were assessed. As mentioned above, to the best of our knowledge, this is the first attempt to exploit two interlaced channels for the growth of cells. Both channels basically showed the same morphologies. The cells spread well and migrated deep into the large pore channels, suggesting the osteoconducting characteristics of the dual-scaffold. More specifically, a large number of cells proliferated favorably on the surfaces of the HA, and the cell membranes were in intimate contact with the HA and well flattened on the surface, as shown in Fig. 8(A, B). These observations indicate that the two interlaced 3-D channels effectively promote the growth of cells.

In addition, it should be noted that the surface area of the dual-scaffold was calculated to be much higher (~2.5 times) than that of a simple 3-D periodic network, comprised of rectangular prisms with the same porosity of 95% and pore size of 500 μm. This result indicates that the dual-scaffold affords a new, simple way of maximizing the surface area of porous materials.

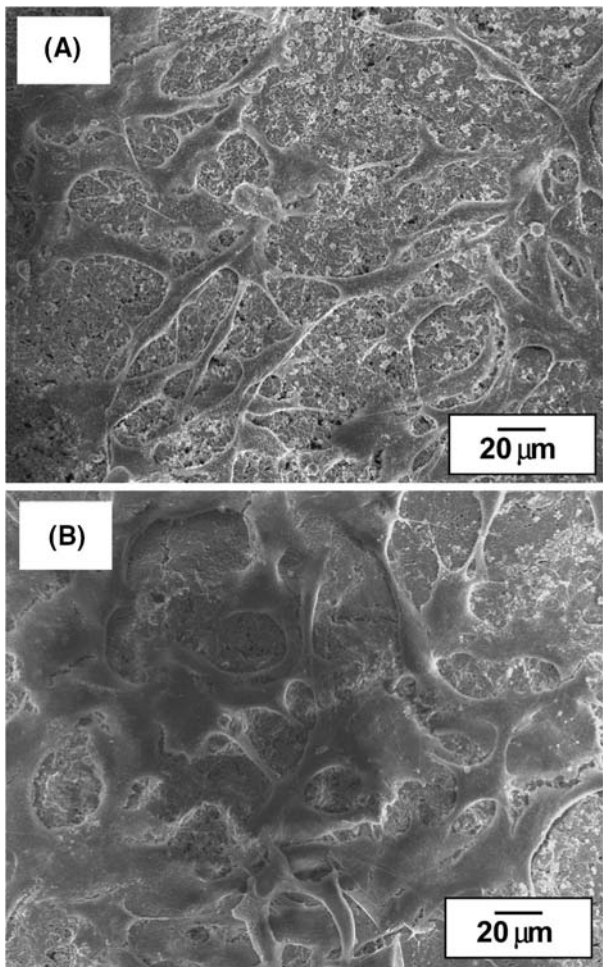

Fig. 8 SEM micrographs illustrating the cell attachments on the surfaces of the HA formed in (**A**) channel I and (**B**) channel II

Conclusions

A novel scaffold for tissue engineering applications, which is referred to as a dual-scaffold, was fabricated by a combination of the rapid prototyping (RP) method and dip-coating process. This dual-scaffold is comprised of two interlaced 3-D channels constructed using two interlaced 3-D HA networks in the form of very thin plates. For the fabrication of this HA dual-scaffold, a 3-D graphite network was prepared as a template using CNC machining and lamination, and then dip-coated with HA slurry. After sintering at 1250 °C for 3 h in air, an additional 3-D channel was newly formed by removing the graphite network, while preserving the pre-existing channel. This fabrication process endowed the HA dual-scaffold with unprecedented features, such as ultra-high porosity, a high surface area, and a high compressive strength, as well as a tightly controlled pore structure. In addition, an excellent cellular response was observed. These results indicate that the HA dual-scaffold should have very useful applications in the tissue engineering field due to its advanced properties.

Acknowledgments This work was supported by a grant from the Korea Health 21 R&D Project, the ministry of Health & Welfare, Republic of Korea (02-PJ3-PG6EV11-0002).

References

1. L. L. HENCH, *J. Am. Ceram. Soc.* **81** (1998) 1705
2. N. PASSUTI, G. DACULSI, J. M. ROGEZ, S. MARTIN and J. V. BAINVEL, *Clin. Orthop. Relat. Res.* **248** (1989) 169
3. J. X. LU, B. FLAUTRE, K. ANSELME, P. HARDOIUN, A. GALLUR, M. DESCHAMPS and B. THIERRY, *J. Mater. Sci.: Mater. Med.* **10** (1999) 111
4. N. O. ENGIN and A. C. TAS, *J. Eur. Ceram. Soc.* **19** (1999) 2569
5. T. M. G. CHU, D. G. ORTON, S. J. HOLLISTER, S. E. Feinberg and J. W. HALLORAN, *Biomaterials* **23** (2002) 1283
6. I. R. GIBSON and W. BONFIELD, *J. Biomed. Mater. Res.* **59** (2002) 697
7. L. L. HENCH and J. M. POLAK, *Science* **295** (2002) 1014
8. K. F. LEONG, C. M. CHEAH and C. K. Chua, *Biomaterials* **24** (2003) 2363
9. S. PADILLA, J. ROMAN and M. VALLET-REGI, *J. Mater. Sci.:Mater. Med.* **13** (2002) 1193
10. F. C. G. de SOUSA and J. R. G. EVANS, *J. Am. Ceram. Soc*. **86** (2003) 517

11. S. CALLCUT and J. C. KNOWLES, *J. Mater. Sci.: Mater. Med*. **13** (2002) 485
12. H. R. RAMAY and M. ZHANG, *Biomaterials* **24** (2003) 3293
13. S. BOSE, J. DARSELL, M. KINTNER, H. HOSICK and A. BANDYOPADHYAY, *Mater. Sci. Eng. C* **23** (2003) 479
14. T. G. M. CHU, J. W. HALLORAN, S. J. HOLLISTER and S. E. FEINBERG, *J. Mater. Sci.: Mater. Med.* **12** (2001) 471
15. J. M. TABOAS, R. D. MADDOX, P. H. KREBSBACH and S. J. HOLLISTER, *Biomaterials* **24** (2003) 181
16. C. E. WILSON, J. D. de BRUIJN, C. A. van BLITTERSWIJK, A. J. VERBOUT and W. J. A. DHERT, *J. Biomed. Mat. Res*. **68A** (2004) 123
17. Y. H. KOH, H. W. KIM, H. E. KIM and J. W. HALLORAN, *J. Mater. Res.* **18** (2003) 2009
18. A. HATTIANGADI and A. BANDYOPADHYAY, *J. Am. Ceram. Soc*. **83** (2000) 2730
19. R. W. RICE, *J. Mater. Sci*. **28** (1993) 2187
20. R. W. RICE, *J. Am. Ceram. Soc.* **76** (1993) 1801
21. H. W. KIM, J. C. KNOWLES and H. E. KIM, *Biomaterials* **25** (2004) 1279